

Circularly polarized electroluminescence in spin-LED structures

Z. G. Yu, W. H. Lau, and M. E. Flatté

Department of Physics and Astronomy, University of Iowa, Iowa City, Iowa 52242

(Dated: November 20, 2018)

We calculate circularly polarized luminescence emitted parallel (vertical emission) and perpendicular (edge emission) to the growth direction from a quantum well in a spin light-emitting diode (spin-LED) when either the holes or electrons are spin polarized. It is essential to account for the *orbital* coherence of the spin-polarized holes when they are captured in the quantum well to understand recent experiments demonstrating polarized edge emission from hole spin injection. The calculations explain many features of the circular polarizations of edge and vertically emitted luminescence for spin polarized hole injection from Mn-doped ferromagnetic semiconductors, and for spin-polarized electron injection from II-VI dilute magnetic semiconductors.

PACS numbers: 72.25.Dc, 72.25.Hg, 72.25.Mk, 85.75.-d.

One of the most widely-used semiconductor spintronic devices [1, 2] is the spin LED[3, 4]. In a spin LED circularly polarized light is emitted after the recombination of spin-polarized carriers that are electrically injected into a semiconductor heterostructure. This device is commonly used to measure the spin injection efficiency into materials[3, 4, 5, 6, 7, 8, 9]. It is therefore vital to quantitatively understand the circular polarization of luminescence (P_ℓ) in order to accurately determine the spin injection efficiency or local spin polarization in a semiconductor. There are two typical spin-LED geometries: the light can come out the edge of the device, or vertically out the top or bottom. As shown in Fig. 1(a) the edge-emitting structures are designed to inject carriers with spin perpendicular to the growth direction, while in Fig. 1(b) the vertical-emitting devices inject carriers with parallel spin. The selection rules for vertical emission are reasonably straightforward – that is not the case for edge emission. A theory based on simple selection rule arguments would suggest zero circular polarization of the edge emission for both electron- and hole-spin injection because of a large energy splitting between heavy- and light-hole states in the typical recombination region, a quantum well (QW). Experiments, however, have demonstrated that although the P_ℓ in Fig. 1(a) is much weaker than in Fig. 1(b), hole-spin injection can lead to a sizable $\sim 1\%$ circular polarization of edge emission[8], although of opposite sign. Meanwhile, reports of edge P_ℓ from electron-spin injection conflict; in a Zener tunneling diode[10] it equals the vertical emission P_ℓ , whereas for a ZnMnSe injector the edge P_ℓ is negligible[11]. Although the selection rules appear more subtle, the device geometry of Fig. 1(a) has important advantages over Fig. 1(b). Large magnetic fields or sophisticated fabrication are generally required to orient the spin out-of-plane [Fig. 1(b)][3, 5, 6, 7, 8, 9]. Hence a quantitative understanding of the origin of polarized edge emission can lead to simpler devices which detect accurately the spin polarization of carriers.

In this letter we resolve many of these discrepancies between the experiments and the theory, by describing

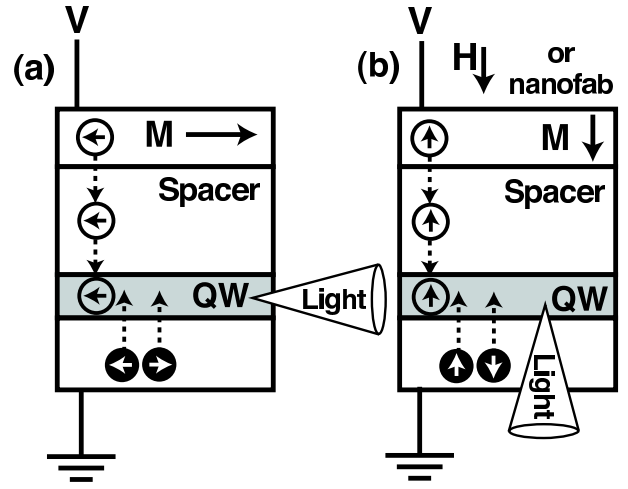


FIG. 1: Schematic showing the spin-LED geometries for edge emission (a) and vertical emission (b). Shape anisotropy tends to force situation (a) without a large vertical magnetic field or nanofabrication.

circularly polarized edge and vertical emission from spin LEDs for both hole- and electron-spin injection within a unified framework that includes the potential for orbital coherence within the QW. The P_ℓ depends on several processes: injection from the magnetic semiconductor into the spacer, transport through the spacer, transport from the spacer to the QW, and the recombination dynamics within the QW. Spin polarization decay lengths within the spacer are seen experimentally to differ significantly depending on the orientation of the hole spins — this is most likely due to anisotropic spin relaxation parallel and perpendicular to carrier motion[12]. Our principal interest is in the question of how the QW luminescence indicates the local spin polarization. Thus we focus on P_ℓ in Fig. 1(a) and (b) for the smallest spacer thickness. A key new ingredient in our theory is that the *orbital* coherence of carriers can be retained when they move from the spacer to the QW. Our calculations can explain many

features of the circular polarizations of edge and vertical emission in spin LED's for hole spin injection from Mn-doped ferromagnetic semiconductors. Due to their orbital degree of freedom, spin-polarized holes give rise to a much stronger edge P_ℓ than spin-polarized electrons.

Edge emission for hole-spin injection [Fig. 1(a)]. The spin LED structure in Ref. [4] consists of a p -type ferromagnetic semiconductor (GaMnAs), a spacer (GaAs), and a QW ($\text{In}_{0.13}\text{Ga}_{0.87}\text{As}$). When spin-polarized holes are injected from the ferromagnetic semiconductor into the spacer, they predominately occupy the heavy-hole states of bulk GaAs. As the orbital quantization axis is parallel to the spin for heavy holes, the states occupied must have a preferred orbital orientation as well, for $|\mathbf{k}\uparrow(\downarrow)\rangle = \frac{1}{\sqrt{V}}|v_{\uparrow(\downarrow)}\rangle e^{i\mathbf{k}\cdot\mathbf{r}}$, where V is the volume, and

$$|v_\uparrow\rangle = \frac{1}{\sqrt{2}}(Y + iZ)|\uparrow_x\rangle, \quad |v_\downarrow\rangle = \frac{1}{\sqrt{2}}(Y - iZ)|\downarrow_x\rangle. \quad (1)$$

Thus for holes, spin polarization selects an orbital wavefunction. The density matrix of holes in the spacer,

$$\rho^h(\mathbf{k}) = f_\uparrow^h(E_{\mathbf{k}})|\mathbf{k}\uparrow\rangle\langle\mathbf{k}\uparrow| + f_\downarrow^h(E_{\mathbf{k}})|\mathbf{k}\downarrow\rangle\langle\mathbf{k}\downarrow|. \quad (2)$$

$f_{\uparrow(\downarrow)}^h(E) = [1 + \exp\{(\mu_{\uparrow(\downarrow)}^h - E)/k_B T\}]^{-1}$ is the Fermi distribution for up-spin (down-spin) holes and $\mu_{\uparrow(\downarrow)}^h$ is the up-spin (down-spin) Fermi energy. The spin polarization of the (non-degenerate) spacer carrier density,

$$P_{d,s} = \frac{e^{\Delta\mu^h/k_B T} - 1}{e^{\Delta\mu^h/k_B T} + 1}, \quad (3)$$

depends on $\Delta\mu^h = \mu_\uparrow^h - \mu_\downarrow^h$.

A 14-band envelope-function $\mathbf{K} \cdot \mathbf{p}$ calculation generates the electronic structure of the QW. Such a calculation accurately predicts the spin splitting in a variety of semiconductor heterostructures[2, 13]. Each eigenstate in the QW is labelled by the momentum \mathbf{K} and an index L for the other quantum numbers.

When the spin-polarized holes move into the QW from the spacer, they would keep their heavy-hole (both orbital and spin) character, $|v_{\uparrow(\downarrow)}\rangle$, if they could. $|v_{\uparrow(\downarrow)}\rangle$ is not an eigenstate in the QW so the holes will relax into QW eigenstates. We describe this relaxation process beginning with a density matrix for holes in the QW,

$$\rho_{LL'}^h(\mathbf{K}, \mathbf{K}') = \phi_{LL'}(\mathbf{K}, \mathbf{K}')|L\mathbf{K}\rangle\langle L'\mathbf{K}'|, \quad (4)$$

$$\begin{aligned} \phi_{LL'}(\mathbf{K}, \mathbf{K}') &= \phi_{LL'}^\uparrow(\mathbf{K}, \mathbf{K}')\langle L\mathbf{K}|v_\uparrow\rangle\langle v_\uparrow|L'\mathbf{K}'\rangle \\ &+ \phi_{LL'}^\downarrow(\mathbf{K}, \mathbf{K}')\langle L\mathbf{K}|v_\downarrow\rangle\langle v_\downarrow|L'\mathbf{K}'\rangle. \end{aligned} \quad (5)$$

This description is central to this paper. It takes into account the wave function overlap between the spacer's (bulk) heavy-hole states $|v_{\uparrow(\downarrow)}\rangle$ and the QW eigenstates $|L\mathbf{K}\rangle$, as well as the carrier distribution function imposed by the spacer (at steady state the spin-dependent electrochemical potentials are continuous across the interface between the spacer and the QW).

If the elastic mean free path of the holes were infinite, only matrix elements that connect states with the same energy in the density matrix would survive, and

$$\phi_{LL'}^{\uparrow(\downarrow)}(\mathbf{K}, \mathbf{K}') = f_{\uparrow(\downarrow)}^h(E_{L\mathbf{K}})\delta(E_{L\mathbf{K}} - E_{L'\mathbf{K}'}). \quad (6)$$

The actual finite scattering rate broadens the delta function in the above equation — here the functional form is assumed to be Gaussian,

$$\begin{aligned} \phi_{LL'}^{\uparrow(\downarrow)}(\mathbf{K}, \mathbf{K}') &= \pi^{-1/2}\alpha^{-1}f_{\uparrow(\downarrow)}^h[(E_{L\mathbf{K}} + E_{L'\mathbf{K}'})/2] \\ &\times \exp[-(E_{L\mathbf{K}} - E_{L'\mathbf{K}'})^2/\alpha^2], \end{aligned} \quad (7)$$

where the parameter α characterizes the scattering rate (assumed equal for all states). In the numerical calculations presented here, α is chosen to be 2 meV, corresponding to a ~ 0.5 ps scattering time. The numerical results are not sensitive to the precise value of α so long as $\alpha \gtrsim 0.1$ meV. The electrons, by contrast, are unpolarized and in equilibrium. Their density matrix,

$$\rho_{\tilde{L}\tilde{L}'}^e(\mathbf{K}, \mathbf{K}') = g_{\tilde{L}\tilde{L}'}(\mathbf{K}, \mathbf{K}')|\tilde{L}\mathbf{K}\rangle\langle\tilde{L}'\mathbf{K}'|. \quad (8)$$

\tilde{L} is the conduction band index, $g_{\tilde{L}\tilde{L}'}(\mathbf{K}, \mathbf{K}') = f^e(E_{\tilde{L}\mathbf{K}})\delta_{\tilde{L}\tilde{L}'}\delta_{\mathbf{K}\mathbf{K}'}$, and $f^e(E) = [1 + \exp(E - \mu^e)]^{-1}$.

The circularly polarized luminescence,

$$\begin{aligned} I_\pm(\omega) &= \sum_{\tilde{L}\tilde{L}'LL', \mathbf{K}, \mathbf{K}'} g_{\tilde{L}\tilde{L}'}(\mathbf{K}, \mathbf{K}')\mathbf{d}_{\tilde{L}'L'}^\pm(\mathbf{K}')\phi_{L'L}(\mathbf{K}', \mathbf{K}) \\ &\times \mathbf{d}_{\tilde{L}\tilde{L}'}^{\pm*}(\mathbf{K}) \delta(\omega - (E_{\tilde{L}\mathbf{K}} + E_{\tilde{L}'\mathbf{K}'} - E_{L\mathbf{K}} - E_{L'\mathbf{K}'})/2), \end{aligned} \quad (9)$$

where $+$ ($-$) represents right- (left-) circular polarization of the light. The matrix elements of the dipole operator

$$\mathbf{d}_{\tilde{L}\tilde{L}'}^\pm(\mathbf{K}) = \langle\tilde{L}\mathbf{K}|\frac{1}{\sqrt{2}}(\mathbf{e}_y \mp i\mathbf{e}_z) \cdot \mathbf{P}|L\mathbf{K}\rangle. \quad (10)$$

As $g_{\tilde{L}\tilde{L}'}(\mathbf{K}, \mathbf{K}')$ is diagonal in the momentum and band index, the \mathbf{K}' and \tilde{L}' sums in Eq. (9) can be done trivially by replacing \mathbf{K}' and \tilde{L}' by \mathbf{K} and \tilde{L} . The circular polarization of luminescence is defined as $P_\ell = (I_+ - I_-)/(I_+ + I_-)$. The spin polarization of density in the QW can be calculated via

$$P_d \equiv \frac{n_\uparrow - n_\downarrow}{n_\uparrow + n_\downarrow} = \langle\sigma_x\rangle = \sum_{LL', \mathbf{K}, \mathbf{K}'} \frac{\text{Tr}[\sigma_x \rho_{LL'}(\mathbf{K}, \mathbf{K}')] }{\text{Tr} \rho_{LL'}(\mathbf{K}, \mathbf{K}')}. \quad (11)$$

Equations (1)-(11) permit orbital coherence to be partially maintained in our calculation — an effect necessary for explaining the edge P_ℓ for hole spin LEDs.

Figure 2(a) shows spectra of the total electroluminescence and the edge P_ℓ for heavy-hole spin injection. The edge emission is circularly polarized and the polarization can easily reach 1%. The maximum circular polarization is 1.4% when fully spin-polarized heavy holes are injected into the spacer ($\Delta\mu^h \rightarrow \infty$). Fig. 2(b) displays the circular polarization of the energy-integrated luminescence and the spin polarization of density as a function of $\Delta\mu^h$.

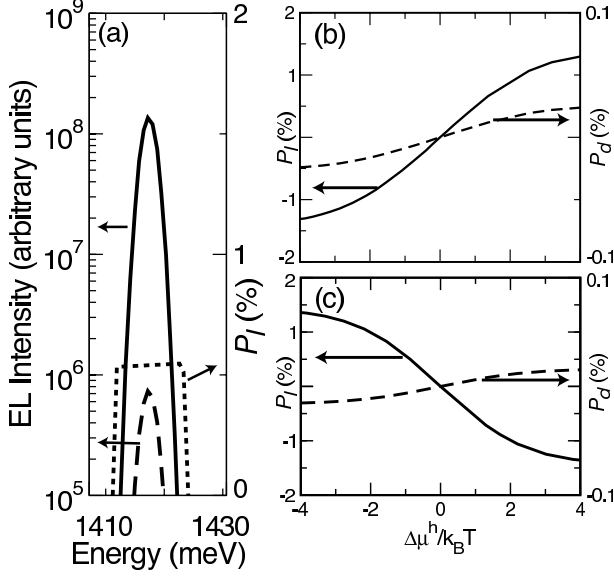


FIG. 2: (a) Total edge emission intensity, $I_+ + I_-$ (thicker solid line), the intensity difference between right-circularly and left-circularly polarized emission, $I_+ - I_-$ (dashed line) and luminescence polarization P_ℓ (dotted line) for heavy-hole spin injection into a 100 Å $\text{In}_{0.13}\text{Ga}_{0.87}\text{As}$ QW with hole density 10^{15} cm^{-3} and $P_{d,s} = 52\%$ ($\Delta\mu^h = 0.57 \text{ meV}$). (b) energy-integrated edge-emission polarization (solid line) and P_d (dashed line) versus $\Delta\mu^h$. (c) same as (b) but for light-hole spin injection. The temperature is 6K. A 3 meV Gaussian linewidth smoothes the luminescence spectrum.

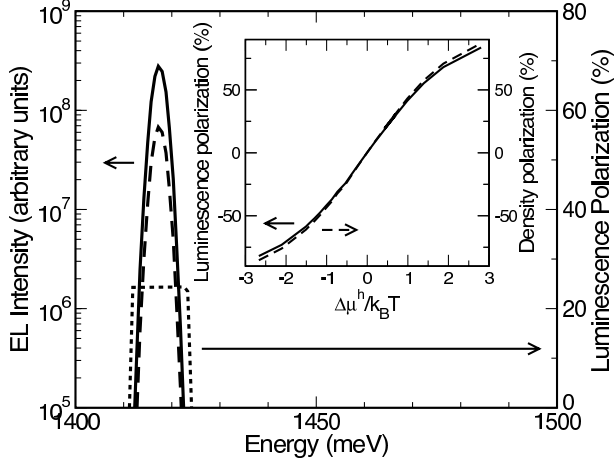


FIG. 3: Vertical emission from the system in Fig. 2(ab) with the same parameters except $P_{d,s} = 27\%$ ($\Delta\mu^h = 0.28 \text{ meV}$).

P_ℓ increases monotonically with $P_{d,s}$, indicating that the edge P_ℓ can be used to accurately measure the spin injection efficiency from the magnetic contact into the spacer. The energy splitting of the heavy holes and light holes in the QW does suppress P_d and P_ℓ relative to $P_{d,s}$. The P_ℓ , however, still greatly exceeds P_d due to the *remnant carrier orbital coherence* in the QW. Figure 2(c) shows

the same quantities as Fig. 2(b), but for light-hole spin injection. The different orbital character of the holes in the spacer leads to a sign reversal of P_ℓ .

Vertical emission for hole spin injection [Fig. 1(b)]. The magnetization of the ferromagnetic semiconductor is now along the z -axis. P_ℓ and P_d can be computed as before by replacing $|v_\uparrow\rangle$ and $|v_\downarrow\rangle$ in Eq. (1) by $|v_\uparrow\rangle = \frac{1}{\sqrt{2}}(X + iY)|\uparrow_z\rangle$ and $|v_\downarrow\rangle = \frac{1}{\sqrt{2}}(X - iY)|\downarrow_z\rangle$, $\mathbf{d}_{LL}^\pm(\mathbf{K})$ in Eq. (10) by $\mathbf{d}_{LL}^\pm(\mathbf{K}) = \langle \tilde{L}\mathbf{K} | \frac{1}{\sqrt{2}}(\mathbf{e}_x \mp i\mathbf{e}_y) \cdot \mathbf{P} | L\mathbf{K} \rangle$, and σ_x in Eq. (11) by σ_z . The spectra of luminescence along the z -axis and P_ℓ are shown in Fig. 3. This configuration leads to a much stronger circular polarization for heavy hole spin injection than the edge-emission configuration, which is consistent with the experimentally observed 14-fold ratio of the circular polarization between the two configurations[8]. Light hole spin injection creates a negligible signal for vertical emission.

The spin and orbital contribution to the emission polarization can be analyzed as a function of momentum \mathbf{K} . The time-reversal symmetry of the system implies that a state $|L\mathbf{K}\rangle$ and its time-reversal state $T|L\mathbf{K}\rangle \rightarrow |\mathcal{L}-\mathbf{K}\rangle$, are related by $E_{L\mathbf{K}} = E_{\mathcal{L}-\mathbf{K}}$. These two states have opposite (pseudo)spin orientations. Noting that $d_{LL}^\pm(\mathbf{K}) = (d_{\mathcal{L}\mathcal{L}}^\mp(-\mathbf{K}))^*$, and the electrons are not spin-polarized, the polarization of light for each momentum \mathbf{K} is

$$\frac{\phi_{LL'}(\mathbf{K}, \mathbf{K}) - \phi_{\mathcal{L}\mathcal{L}'}(-\mathbf{K}, -\mathbf{K})}{\phi_{LL'}(\mathbf{K}, \mathbf{K}) + \phi_{\mathcal{L}\mathcal{L}'}(-\mathbf{K}, -\mathbf{K})} = \mathcal{D}_{LL'}(\mathbf{K})W_{LL'}(\mathbf{K}), \quad (12)$$

where

$$\mathcal{D}_{LL'}(\mathbf{K}) = \frac{f_\uparrow^h[(E_{L\mathbf{K}} + E_{L'\mathbf{K}})/2] - f_\downarrow^h[(E_{L\mathbf{K}} + E_{L'\mathbf{K}})/2]}{f_\uparrow^h[(E_{L\mathbf{K}} + E_{L'\mathbf{K}})/2] + f_\downarrow^h[(E_{L\mathbf{K}} + E_{L'\mathbf{K}})/2]}$$

$$W_{LL'}^h(\mathbf{K}) = \frac{\langle L\mathbf{K} | v_\uparrow \rangle \langle v_\uparrow | L'\mathbf{K} \rangle - \langle L\mathbf{K} | v_\downarrow \rangle \langle v_\downarrow | L'\mathbf{K} \rangle}{\langle L\mathbf{K} | v_\uparrow \rangle \langle v_\uparrow | L'\mathbf{K} \rangle + \langle L\mathbf{K} | v_\downarrow \rangle \langle v_\downarrow | L'\mathbf{K} \rangle}. \quad (13)$$

Thus the P_ℓ is determined not only by $\Delta\mu^h$ but also the characteristics of the wave functions in the spacer and in the QW. For vertical emission the character of the QW eigenstates at the top of the valence band is very similar to the polarized heavy-hole states in the spacer, so $W_{LL'}^h$ is close to $\pm\delta_{LL'}$ and $P_\ell \approx P_{d,s}$. For edge emission the process is more complex. First, holes are spin polarized in the spacer (characterized by $\mathcal{D}_{LL'}$). This spin polarization in the spacer is converted to a predominately orbital coherence in the QW (off-diagonal components of $W_{LL'}^h$), which produces circularly polarized luminescence.

For larger hole densities in the QW the carriers will occupy QW eigenstates with higher energies and different character. Figure 4(inset) shows the edge emission and the circular polarization for fully polarized ($\Delta\mu^h \rightarrow \infty$) holes with density 10^{16} cm^{-3} . A new peak emerges at a higher energy in the luminescence spectrum. The circular polarization at the high-energy peak has the opposite sign as that of the low-energy peak, suggesting that the injected holes may begin to enter QW states with light-hole character. The energy-integrated circular polarization over the low-energy peak region, however, is

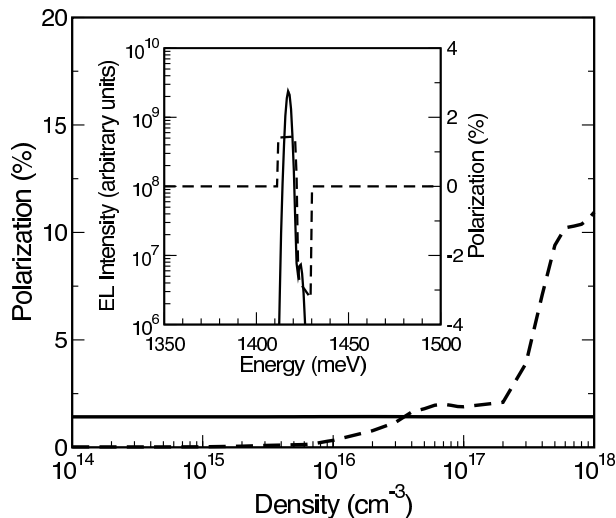


FIG. 4: Maximal P_ℓ (solid line) and P_d (dashed line) in the QW as a function of hole density for in-plane emission at $T = 6\text{K}$. The inset illustrates the total electroluminescence (solid line) and P_ℓ with hole density 10^{16} cm^{-3} .

independent of the carrier density over the entire experimentally accessible range, as illustrated in Fig. 4. This agrees with the measured insensitivity of P_ℓ to the current. Figure 4 also shows that P_d increases with the total hole density in the QW (states with light-hole characteristics can, with the heavy holes, form a state with spin along the x -axis).

Emission from electron spin injection. The wavefunctions of injected electrons in the spacer region are $|k \uparrow (\downarrow)\rangle = \frac{1}{\sqrt{V}}|c_{\uparrow(\downarrow)}\rangle e^{i\mathbf{k}\cdot\mathbf{r}}$, $|c_{\uparrow(\downarrow)}\rangle = |S_{\uparrow_x(\downarrow_x)}\rangle$ for the in-plane configuration and $|c_{\uparrow(\downarrow)}\rangle = |S_{\uparrow_z(\downarrow_z)}\rangle$ for the z -axis configuration. The density matrix of electrons is constructed as in Eq. (5) with $|v_{\uparrow(\downarrow)}\rangle$ substituted by $|c_{\uparrow(\downarrow)}\rangle$. The holes are unpolarized and only the diagonal elements in the hole density matrix have nonzero values. As the electrons have no orbital degree of freedom comparable to that of the heavy holes, the expectations for edge emission should be very different.

The P_ℓ and P_d in the QW as a function of the Fermi-energy splitting for both edge- and vertical-emission configurations are shown in Fig. 5. The P_ℓ for electron-spin injection is very weak, at least one order of magnitude smaller than that for hole spin injection. This is in agreement with recent experiments of II-VI spin-LED structures using electron spin injection[11], but not with mea-

surements on Zener tunneling diodes[10]. Despite the low P_ℓ , electrons in the QW can be fully polarized along the x -axis. The large P_d along the x -axis occurs because the spin-up and spin-down states in the conduction band are still nearly degenerate and a state with $|c_{\uparrow_x(\downarrow_x)}\rangle$ characteristics can be constructed from states with $|c_{\uparrow_z(\downarrow_z)}\rangle$ characteristics. The vertical-emission electron spin LED can have a strong circular polarization, and $P_\ell \approx P_{d,s}$.

Circularly polarized luminescence has been calculated from spin LEDs for both hole- and electron-spin injection.

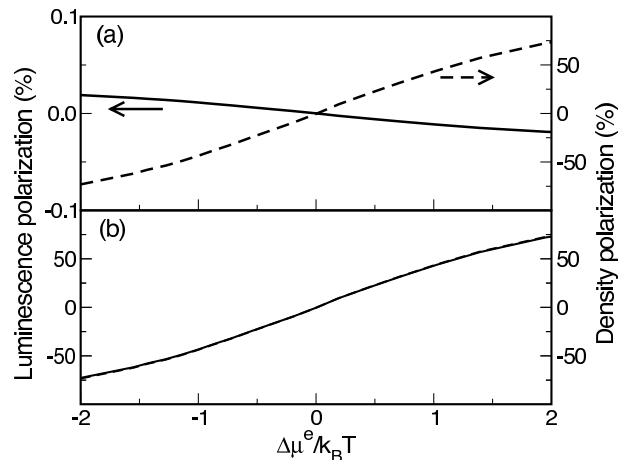


FIG. 5: Luminescence and density polarizations versus the Fermi-level splitting for spin-LED structures using spin-polarized electrons. Panels (a) and (b) are for edge emission and vertical emission, respectively. The solid lines describe the luminescence polarization and the dashed lines describe the density polarization. The electron density is 10^{15} cm^{-3} and the temperature is 6 K.

When spin-polarized carriers move from the spacer to the QW, they try to maintain their *orbital* coherence. Our calculations can explain many features of the circular polarizations of both edge and vertical emission observed in Mn-doped ferromagnetic semiconductor spin LEDs. Our results also indicate that spin-polarized holes give rise to a much stronger in-plane circular polarization of luminescence than do spin-polarized electrons, consistent with the experimental measurements of II-VI spin LEDs using spin polarized electrons.

This work was supported by DARPA/ARO DAAD19-01-0490.

-
- [1] See, e.g., S. A. Wolf *et al.*, Science, **294**, 1488 (2001), and references therein.
 [2] *Semiconductor Spintronics and Quantum Computation*, ed. D. D. Awschalom, N. Samarth, and D. Loss, Springer, New York, 2002.
 [3] R. Fiederling *et al.*, Nature (London) **402**, 787 (1999).

- [4] Y. Ohno *et al.*, Nature (London) **402**, 790 (1999).
 [5] B. T. Jonker *et al.*, Phys. Rev. B **62**, 8180 (2000).
 [6] H. J. Zhu *et al.*, Phys. Rev. Lett. **87**, 016601 (2001).
 [7] A. F. Isakovic *et al.*, Phys. Rev. B **64**, 161304(R) (2001).
 [8] D. K. Young *et al.*, Appl. Phys. Lett. **80**, 1598 (2002).
 [9] A. T. Hanbicki, *et al.*, Appl. Phys. Lett. **80**, 1240 (2002).

- [10] D. K. Young, *et al.*, *Semicond. Sci. Technol.* **17**, 275 (2002).
- [11] R. Fiederling *et al.*, *Appl. Phys. Lett.* **82**, 2160 (2003).
- [12] S. J. Papadakis, E. P. De Poortere, M. Shayegan, and R. Winkler, *Phys. Rev. Lett.* **84**, 5592 (2000).
- [13] W. H. Lau, J. T. Olesberg, and M. E. Flatté, *Phys. Rev. B* **64**, 161301 (R) (2001).